NASA TN D-1192

TECHNICAL NOTE
D-1192

DETERMINATIONS OF LOCAL AND INSTANTANEOUS COMBUSTION CONDITIONS FROM ACOUSTIC MEASUREMENTS IN A ROCKET COMBUSTOR AND COMPARISON WITH OVERALL PERFORMANCE

By Martin Hersch

Lewis Research Center
Cleveland, Ohio

NATIONAL AERONAUTICS AND SPACE ADMINISTRATION
WASHINGTON
March 1962

NATIONAL AERONAUTICS AND SPACE ADMINISTRATION

TECHNICAL NOTE D-1192

DETERMINATIONS OF LOCAL AND INSTANTANEOUS COMBUSTION CONDITIONS FROM ACOUSTIC MEASUREMENTS IN A ROCKET COMBUSTOR AND COMPARISON WITH OVERALL PERFORMANCE

By Martin Hersch

SUMMARY

Local instantaneous combustion conditions and the characteristic exhaust velocity were measured for a hydrogen-oxygen combustor. The combustion conditions of the chamber gases were determined from the transit time required for ultrasonic pulses to travel across the combustion chamber. Approximately 300 pulses were made per second. The characteristic exhaust velocity was measured in the conventional manner.

The propellants were gaseous hydrogen - gaseous oxygen and gaseous hydrogen - liquid oxygen. The combustor had a nominal thrust of 100 pounds. The experimental variables were the injection state of the oxygen (liquid or gaseous) and the oxidant-fuel ratio. The oxidant-fuel ratio was varied from 3.2 to 10.0 at a chamber pressure of approximately 200 pounds.

Both the time-averaged sound velocity and instantaneous velocities obtained from separate pulses were studied. The time-averaged sound velocity efficiency (ratio of experimental to theoretical value) was found to increase with increasing oxidant-fuel ratio, reaching a maximum at an oxidant-fuel ratio of about 6.0 for liquid oxygen and 8.0 for gaseous oxygen. The sound velocity efficiency decreased slightly with further increases of the oxidant-fuel ratio. The characteristic exhaust velocity followed a similar trend with liquid oxygen, but was almost independent of oxidant-fuel mixture ratio when gaseous oxygen was used.

The variation of sound velocity during each run was studied in order to determine the presence of combustion fluctuations and time-varying gas inhomogeneities. The analysis of these data indicated that the gases were more homogeneous at the higher oxidant-fuel ratios and with gaseous oxygen.

INTRODUCTION

A conventional index of rocket combustor performance and combustion efficiency is the characteristic exhaust velocity calculated from chamber pressure, nozzle throat area, and propellant weight flows. This is a time-averaged value for the entire chamber-nozzle combination and does not directly convey information about local burning conditions at various stations along the chamber. Knowledge of the local conditions is important because it may improve understanding of time-averaged performance and combustion instability; the information itself may prove to be a valuable input for analyses of steady-state combustion and nonlinear instability analyses (refs. 1 and 2). At present, information about local conditions is inferred by comparing the performance of short chambers with that of long ones and is also derived from photographic data as described in reference 3.

This report describes a technique developed to measure instantaneous and local combustion conditions in a rocket combustor and compares those measurements with experimental average characteristic exhaust velocity values at various operating conditions. The technique is based on the fact that the sound velocity of gases may be used as measure of their temperature and composition. The speed of sound of the combustion gases was obtained by measuring the time required for acoustic pulses to travel across a path of known length in the combustor chamber; the approach is similar to those reported in references 4 and 5 for studying combustion in reciprocating internal combustion engines. In this report "instantaneous" refers to a measurement made in a time interval that is small compared with the stay-time of the gas in the combustor; thus, the traverse time for an acoustic pulse was 15 to 35 microseconds compared with a stay-time of the order of a millisecond. The term "local" refers to a measurement zone whose volume is small compared with the total combustor volume; thus, the 1/4-inch-diameter acoustic beam traversed a volume of about 0.036 cubic inch compared with a combustor volume in excess of 20 cubic inches.

The measurements were made in a nominal 100-pound-thrust "two-dimensional" hydrogen-oxygen engine. Both liquid and gaseous oxygen were used as the oxidant. The fuel was gaseous hydrogen. The oxidant-fuel ratio of the engine was varied from 3.2 to 10.0.

APPARATUS

Combustor

A diagram of the combustor used for this study is shown in figure 1. The overall length was $10\frac{1}{2}$ inches including a 3-inch-long nozzle. The

combustion chamber was 3.33 inches wide and 3/4 inch thick. A portion of the chamber was water-cooled and contained ultrasonic transducers located $5\frac{1}{2}$ inches downstream of the injector. The nozzle was circular, with a throat diameter of 0.75 inch and a contraction ratio of 5.65. A sparkplug was used for ignition.

Injector

The oxygen injector was of the parallel-jet type and, by a change of injector plate, could handle either liquid or gaseous oxygen. The liquid plate contained 39 holes 0.0180 inch in diameter spaced 0.220 inch apart arranged in three parallel rows equally spaced 0.188 inch apart. The plate for gaseous oxygen had one row of thirteen 0.1405-inch-diameter holes equally spaced 0.220 inch apart. The plates were 1/4 inch thick.

The hydrogen was injected through two 1/2-inch tubes at right angles to the combustor axis, immediately below the oxygen injector plate, as indicated in figure 1.

Electronic System and Transducers

A schematic diagram of the electronic system used to measure the sound velocity is shown in figure 2. The system consisted of a tunable continuous-wave generator whose output was pulsed by a square-wave generator. This pulsed signal was then applied simultaneously to the transmitting transducer mounted in the combustor wall (fig. 1) and to the upper beam of a two-beam oscilloscope. The transmitting transducer, shown in figure 3, converted this electrical signal to an acoustic signal that traveled through the combustion gases. It was then reconverted to an electrical signal by the receiving transducer mounted directly opposite the transmitting transducer. This signal, after passing through a bandpass filter tuned to the signal generator frequency, was applied to the lower beam of the oscilloscope. The transmitted signal triggered the common sweep of the oscilloscope. The received signal, which suffered a time delay in traveling through this system, including the delay in traveling through the combustion gases, was displaced on the oscilloscope screen relative to the transmitted signal by a distance proportional to this time delay.

The carrier frequency within the pulses was tuned to produce a maximum acoustic signal. This frequency was usually between 150 to 170 kilocycles per second. The pulse repetition rate was about 300 pulses per second, with a pulse length of about 80 microseconds. Time-delay measurements were made from corresponding points on the pulse envelope rather than from corresponding waves within the pulses. Therefore, it was the group velocity rather than the phase velocity that was measured.

Transducers

The transmitting and receiving transducers were identical. The transducers (fig. 3) consisted, essentially, of a piezoelectric crystal and an aluminum transmission rod $2\frac{1}{4}$ inches long which acoustically coupled the crystal to the combustion gases and shielded the crystals from the high combustion temperatures. Teflon washers and rubber O-rings were used to provide acoustic isolation and sealing of the probes. Because of the very short run time (1.5 sec) the probes were not cooled. The piezoelectric crystals, a lead zirconate titanate ceramic, were 1/2 inch in diameter and 0.10 inch thick. The ends of the transmitting rods in contact with the combustion gases were 1/4 inch in diameter.

Combustor Performance

Combustor performance was evaluated in terms of characteristic exhaust velocity c*, which was calculated from measurements of chamber pressure, propellant flow rates, and the nozzle throat area.

Chamber pressure was measured by means of a strain-gage-type transducer. Liquid-oxygen flow was measured with a rotating-vane-type flowmeter, whose output was converted to a d-c voltage. Gaseous-propellant flows were measured with standard ASME critical flow orifices.

With this system the random error in c* values was approximately $\pm 2\frac{1}{2}$ percent. The run duration was about 1.5 seconds.

Instantaneous Local Combustion Measurements

Instantaneous local combustion conditions were determined by measuring the delay time between the transmitted and received electrical signals. This delay time was composed of two parts: First, the fixed delay time due to the electronic circuitry and transmission rods; and second, the continuously variable delay due to the time for the ultrasonic signal to travel through the combustion gases.

The fixed time delay, which was about 30 microseconds, was determined from measurements of the total time delay when a gas of known sound velocity, either static (nonflowing) hydrogen or nitrogen, was present between the transducers. This fixed time was measured each day from direct, visual observations of the oscilloscope signal. The values of the fixed transit time measurements using different static calibrating gases agreed with each other to within $\pm 3\frac{1}{2}$ percent.

Time delays during combustion were obtained by photographing the oscilloscope screen with a moving film strip camera. The film speed and pulse repetition rate were adjusted so that individual oscilloscope sweeps could be resolved. Examples of typical oscillograms during combustion are shown in figure 4. The time delays of each readable pulse were determined with the aid of a film analyzer. The sound velocity was calculated using the following equation:

$$U = \frac{L}{k\,\Delta d - t_k}$$

where

U velocity of sound, ft/sec

L distance traversed by ultrasonic signals in combustor, ft

k ratio of time scale of oscilloscope to distance as read on film analyzer, sec/in.

Δd distance, as read on film analyzer, from start of trace to leading edge of received pulse, in.

t_k fixed time delay due to electronic circuits and transmission rods, sec

The maximum estimated errors in values of L, k, d, and t_k were approximately ±0.1, ±4, ±1, and ±3 percent, respectively. However, on some traces, because of noise and signal absorption in the combustion gases, the leading edge of the received pulse was not clearly defined. These signals were not used for measurements. Another source of error is that due to the velocity of the combustion gases, which is perpendicular to the ultrasonic beam, thus causing a downstream displacement of the ultrasonic signal. However, this is a negligible effect because the velocity of the chamber gases is much less than the speed of sound.

As a test of the accuracy of this technique, instantaneous measurements were made of cold flowing hydrogen. The average value of the measurements was found to agree with that given in the literature to ±2 percent, with 50 percent of the number of measurements being within ±6 percent of the average value. It is therefore concluded that the probable error of the sound velocity using this technique is ±6 percent.

RESULTS AND DISCUSSION

The experimental characteristic exhaust velocities and time-averaged sound velocities are listed in table I as both absolute values and as percentage of theoretical values (efficiencies). The theoretical values of characteristic exhaust velocity as a function of oxidant-fuel mixture ratio were calculated for equilibrium composition conditions at the throat and are shown in figure 5. The theoretical sound velocity as a function of oxidant-fuel mixture ratio was calculated for frozen composition conditions in the chamber and is shown in figure 6. The speed of sound for frozen and equilibrium composition differed only in the value of the specific-heat ratio. The data of table I, as presented in figure 7, indicate that both characteristic exhaust velocity efficiency and time-averaged sound velocity efficiency increase with increasing oxidant-fuel ratio, reach a maximum, and then decrease slightly. This effect, however, is less pronounced for gaseous oxygen than for liquid oxygen. This effect also shows up more strongly for the sound velocity efficiency than for the characteristic exhaust velocity efficiency.

The characteristic exhaust velocity c^* may be expressed as a function of sound velocity and specific heat ratio, as shown in reference 6 and in the following expression:

$$c^* = \frac{a}{\gamma\sqrt{\left(\frac{2}{\gamma+1}\right)^{\frac{\gamma+1}{\gamma-1}}}}$$

where

a velocity of sound, ft/sec

γ ratio of specific heat at constant pressure to specific-heat ratio at constant volume

Therefore, sound velocity measurements may be used to determine c^* efficiency. Figure 8 shows theoretical sound velocity as a function of metered oxidant-fuel ratio with c^* efficiency as a parameter. This relation was obtained by calculating the sound velocity and specific-heat ratio for hydrogen-oxygen combustion assuming various portions of the oxygen to be unreacted. For calculation purposes the unreacted oxygen was treated as an inert gas and was considered to be a heat sink. These calculations were made for a number of metered oxidant-fuel ratios. Figure 8 was then used to convert the sound velocity data of table I into the local c^* efficiency points shown in figure 9. A faired curve was then drawn through these points.

Figure 9 shows the relation of overall performance to a local performance as determined from sound velocity measurements upstream of the nozzle. It is seen that the local efficiency and overall efficiency show a parallel trend with oxidant-fuel mixture ratio. The local efficiency, however, is always lower than that which is measured at the nozzle, as would be anticipated, since the local efficiency was determined at a point $5\frac{1}{2}$ inches downstream in a $10\frac{1}{2}$-inch-long chamber-nozzle.

Varporization calculations, using the method of reference 1 and the experimental conditions of this study, indicate that over 99 percent of the oxygen should theoretically have been vaporized at a station $5\frac{1}{2}$ inches downstream of the injector, over the entire experimental oxidant-fuel mixture ratio. It may therefore be concluded that the increase of performance in the final 5 inches of chamber and nozzle length shown in figure 9 is due to a continuation of mixing and burning, rather than vaporization.

A typical distribution of sound velocity measurements for a single run is shown in figure 10. The data for all the runs approximated those of a normal distribution. Included in this figure are the sound velocity of completely reacted combustion gases having a metered oxidant-fuel ratio equal to that of this run, and the maximum sound velocity possible for gaseous-hydrogen - liquid-oxygen combustion, which corresponds to a metered oxidant-fuel ratio of 2.0. Also shown are sound velocities for hydrogen gas at the injection temperature and at 1000° K.

This range of experimental sound velocity indicated in figure 10 suggests that the combustion gases may have been burning at oxidant-fuel ratios greatly different from the metered value. The very low values may have been caused by cool, unreacted gases of high molecular weight. Values of sound velocity greater than the maximum possible for hydrogen-oxygen combustion could only be caused by the presence of hot hydrogen-rich gas. This distribution of sound velocity would seem to indicate that the combustion gases were not uniform, but consisted of random pockets in various states of mixing and burning.

The geometric standard deviation of the sound velocity measurements was computed for each run and is shown as a function of oxidant-fuel ratio in figure 11. The standard geometric deviation is a measure of variation of sound velocity and also, therefore, a measure of the uniformity of the combustion gases. The curves, drawn through the points of this figure, show a tendency of the standard deviation to decrease as the oxidant-fuel mixture ratio was increased. This may be interpreted as an increase of combustion gas uniformity with increasing oxidant-fuel mixture ratio at the location in the chamber at which the measurements were made. This may be a possible explanation for the increase of overall performance with

increasing oxidant-fuel mixture ratio. The standard deviation is also slightly lower for the gaseous system, which indicates more uniform burning when liquid oxygen is replaced by gaseous oxygen. The similarities, however, of these sets of data suggest that the same mechanisms that limited the performance of the liquid system also limited that of the gaseous system. It is improbable therefore that the performance of the liquid system was vaporization-rate-limited.

The standard geometric deviation of cold-flowing hydrogen gas is also shown in figure 11. Although this was chemically a uniform gas, the standard geometric deviation of the sound velocity was greater than one. This may have been due to turbulence and noise caused by flow. The standard deviation is lower though than any of the combustion results. This demonstrates that the geometric standard deviation of sound velocity measurements may be used as a measure of the uniformity of combustion.

SUMMARY OF RESULTS

The velocity of sound of chamber combustion gases and the overall characteristic exhaust velocity were measured for a hydrogen-oxygen rocket combustor. The sound velocity measurements were used to determine both local time averaged and instantaneous combustion conditions upstream of the nozzle. The following results were obtained:

1. Distribution of sound velocity during individual runs indicated the heterogeneous, fluctuating nature of the combustion gases. The gases appeared to be more uniform when gaseous oxygen replaced the liquid oxygen. The gases also appeared to be more uniform at higher oxidant-fuel mixture ratios.

2. Overall performance measurements and results of sound velocity measurements indicated that, even with complete vaporization, a relatively long chamber may be needed to permit attainment of a high combustion efficiency.

3. Local efficiencies obtained with sound velocity measurements $5\frac{1}{2}$ inches downstream were always lower than the efficiency measured at the nozzle. This increase in performance in the remainder of the chamber appeared to be due to a continuation of mixing and burning rather than vaporization.

4. The local characteristic exhaust velocity, as determined from sound velocity measurements, was found to increase with increasing oxidant-fuel mixture ratio, reach a maximum at about 6 with liquid oxygen and 8 with gaseous oxygen, and decreased slightly with further increases in oxidant-fuel mixture ratio. The overall performance with gaseous

oxygen followed the same trend with oxidant-fuel mixture ratio as did the local performance, but the performance with gaseous oxygen was almost independent of the oxidant-fuel mixture ratio.

Lewis Research Center
National Aeronautics and Space Administration
Cleveland, Ohio, November 22, 1961

E-1507

REFERENCES

1. Priem, Richard J., and Heidmann, Marcus F.: Propellant Vaporization as a Design Criterion for Rocket-Engine Combustion Chambers. NASA TR R-67, 1960.

2. Priem, Richard J.: A Non-Linear Treatment of Combustion Instability. Paper presented at JANAF-NASA-ARPA Liquid Propellant Group Meeting, Miami (Fla.), Nov. 7-9, 1961.

3. Clark, Bruce J., Hersch, Martin, and Priem, Richard J.: Propellant Vaporization as a Criterion for Rocket-Engine Design; Experimental Performance, Vaporization, and Heat-Transfer Rates with Various Propellant Combinations. NASA MEMO 12-29-58E, 1959.

4. Livengood, J. C., Rona, T. P., and Baruch, J. J.: Ultrasonic Temperature Measurement in Internal Combustion Engine Chamber. Jour. Acoustical Soc. Am., vol. 26, no. 5, Sept. 1954, pp. 824-830.

5. Zelda, E. T.: End-Gas Temperature Monitor. IM-4, Ethyl Corp., May 1958.

6. Sutton, George P.: Rocket Propulsion Elements. Second ed., John Wiley & Sons, Inc., 1956.

TABLE I. - EXPERIMENTAL DATA AND RESULTS

Oxidant-fuel ratio	Oxidant flow, lb/sec	Fuel flow, lb/sec	Total flow, lb/sec	Chamber pressure, lb/sq in. abs	Experimental characteristic exhaust velocity		Experimental sound velocity, time averaged	
					ft/sec	% theoretical	ft/sec	% theoretical
Gaseous hydrogen - liquid oxygen								
3.20	0.442	0.138	0.580	245	7230	87.4	3470	57.4
3.54	.442	.125	.567	240	7250	88.1	3830	64.6
4.02	.455	.113	.568	235	7070	87.0	3910	67.4
4.27	.417	.0977	.515	245	8140	101	4720	82.4
4.77	.422	.0833	.510	240	8040	101	4840	86.4
5.21	.442	.0849	.527	245	7950	102	5270	95.9
5.91	.455	.0770	.532	245	7870	103	4880	91.6
6.94	.499	.0772	.571	245	7340	100	4420	86.6
7.22	.555	.0770	.632	235	6350	87.6	4050	80.4
7.27	.513	.0706	.583	245	7220	99.4	4780	87.2
Gaseous hydrogen - gaseous oxygen								
3.94	0.278	0.0706	0.355	178	7160	87.1	4300	73.5
4.58	.328	.0700	.390	198	7260	90.0	4770	84.4
5.00	.350	.0700	.420	209	7130	90.0	4530	81.5
5.84	.408	.0700	.478	231	6900	89.5	4660	87.0
5.84	.408	.0700	.478	233	6970	90.5	4230	78.9
6.00	.427	.0710	.498	235	6750	88.3	4570	85.3
6.55	.460	.0700	.530	247	6660	88.9	4580	88.1
6.80	.428	.0630	.491	227	6610	89.2	4490	87.1
7.24	.517	.0715	.589	263	6400	87.7	4870	96.4
7.60	.537	.0710	.608	275	6460	89.7	4220	85.3
7.73	.530	.0685	.599	271	6470	90.2	4890	99.7
7.84	.435	.0555	.490	219	6400	89.7	4290	87.5
8.25	.598	.0725	.671	292	6220	88.5	4270	88.9
8.33	.595	.0715	.667	289	6190	88.4	4640	96.7
8.70	.456	.0524	.508	219	6170	89.1	4120	87.7
10.0	.456	.0455	.502	209	6520	89.6	3914	89.0

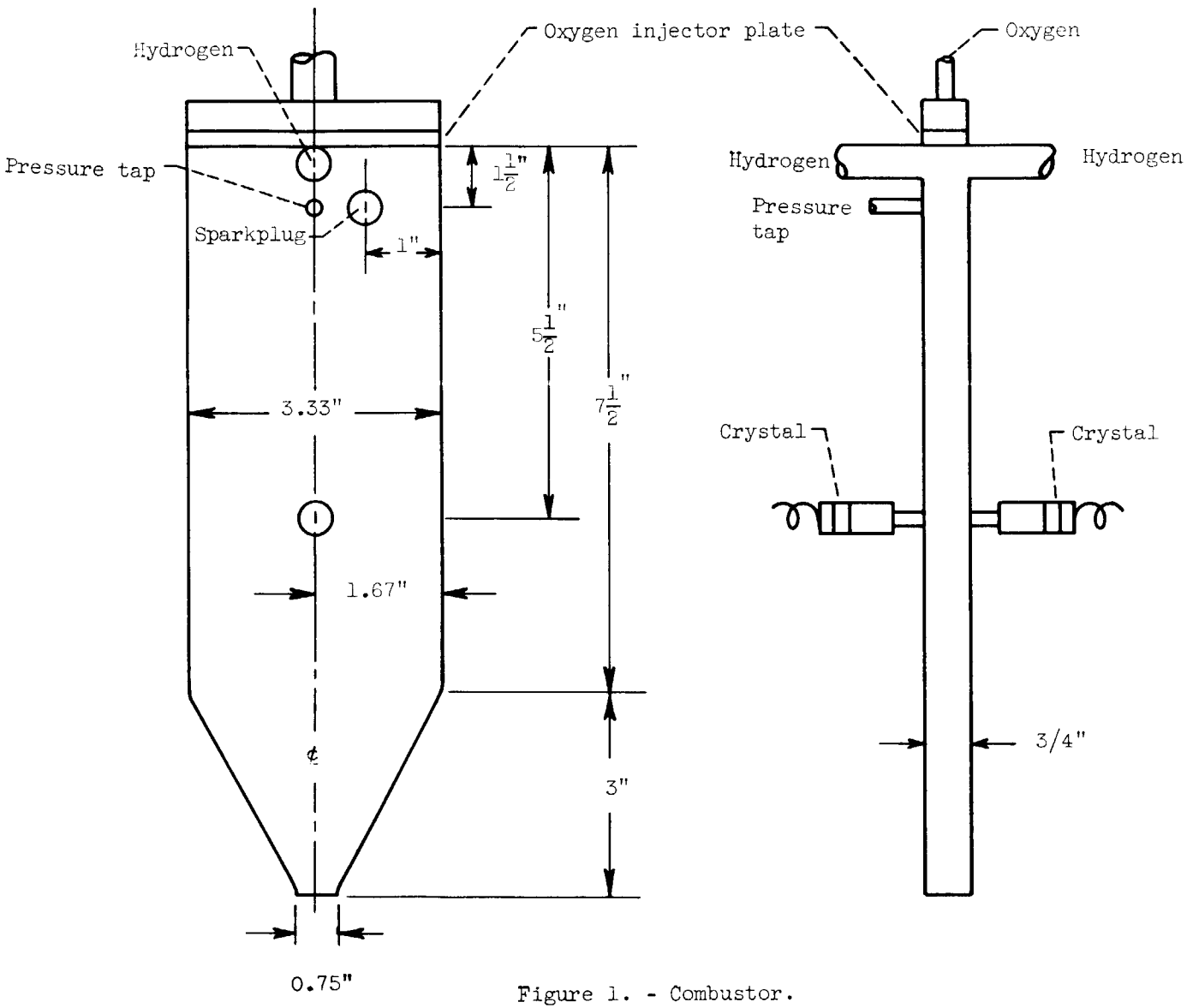

Figure 1. - Combustor.

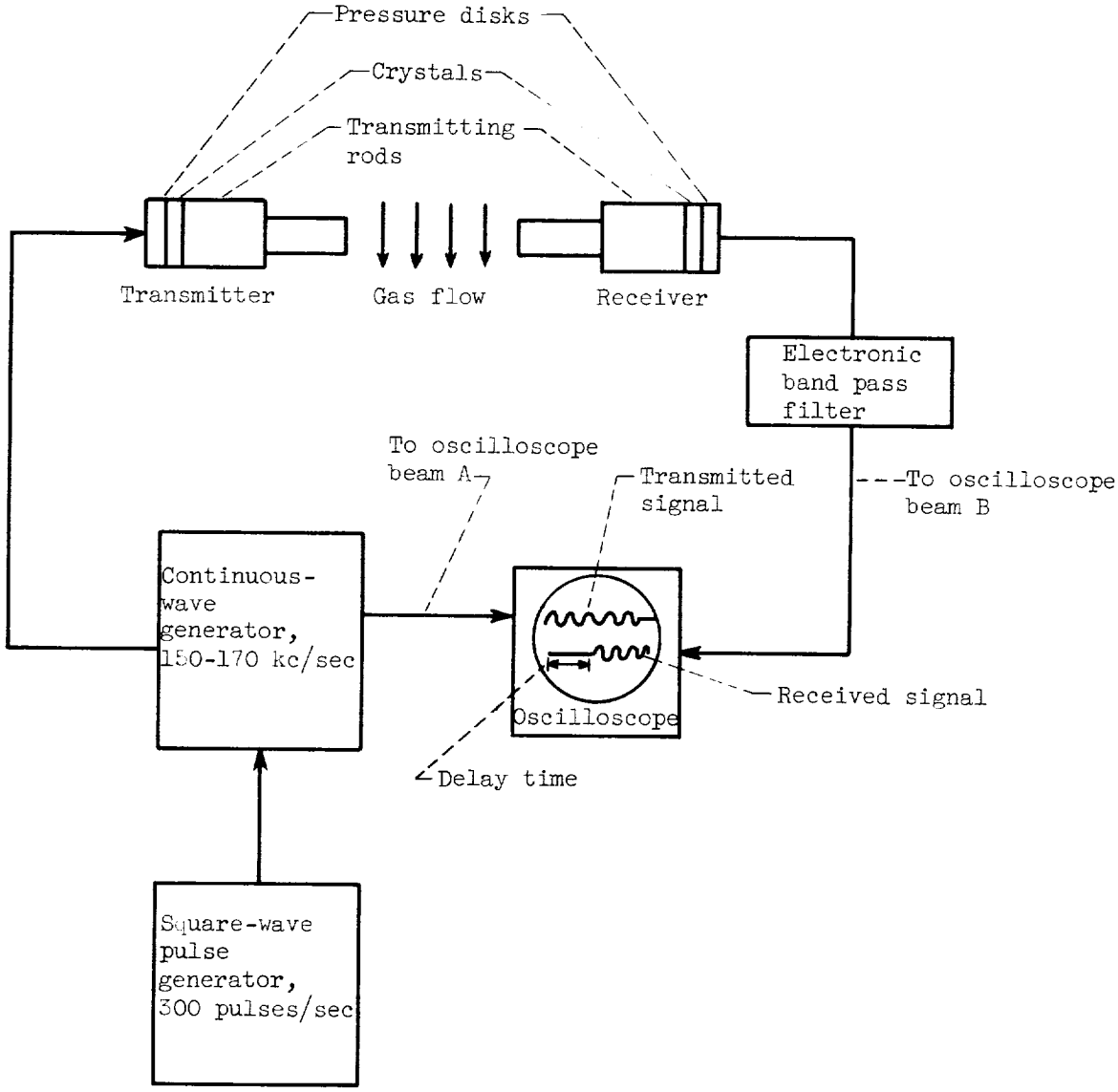

Figure 2. - Schematic diagram of sound velocity method.

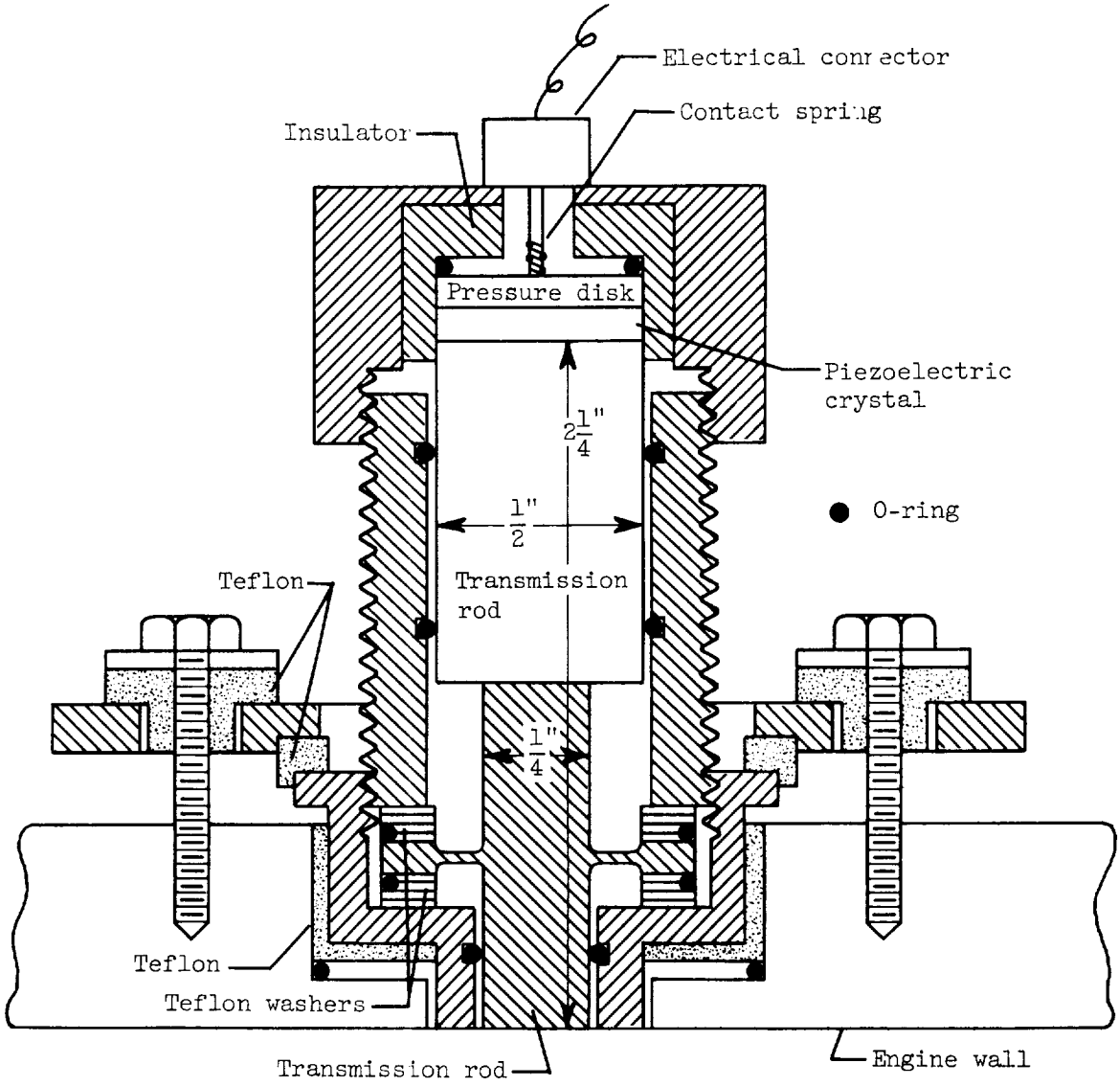

Figure 3. - Detail of receiving and transmitting transducer.

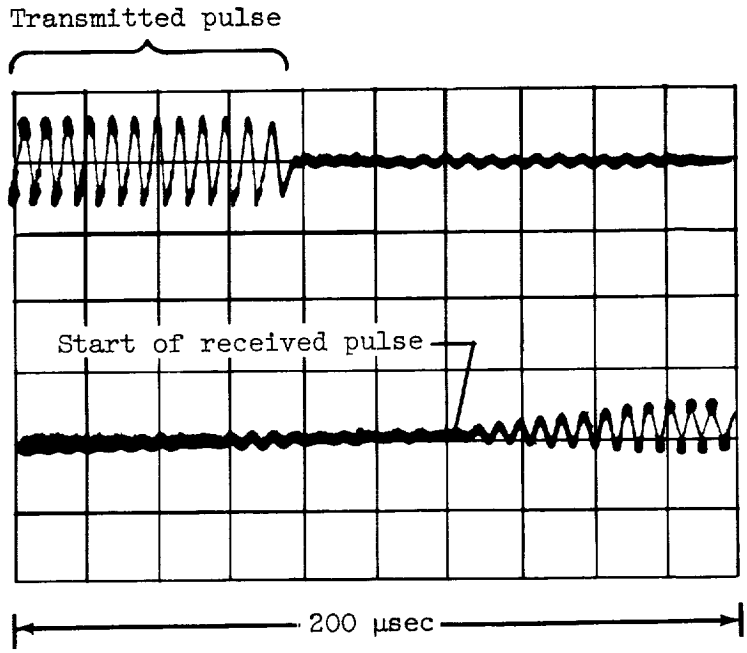

Figure 4. - Typical example of oscilloscope trace during combustion.

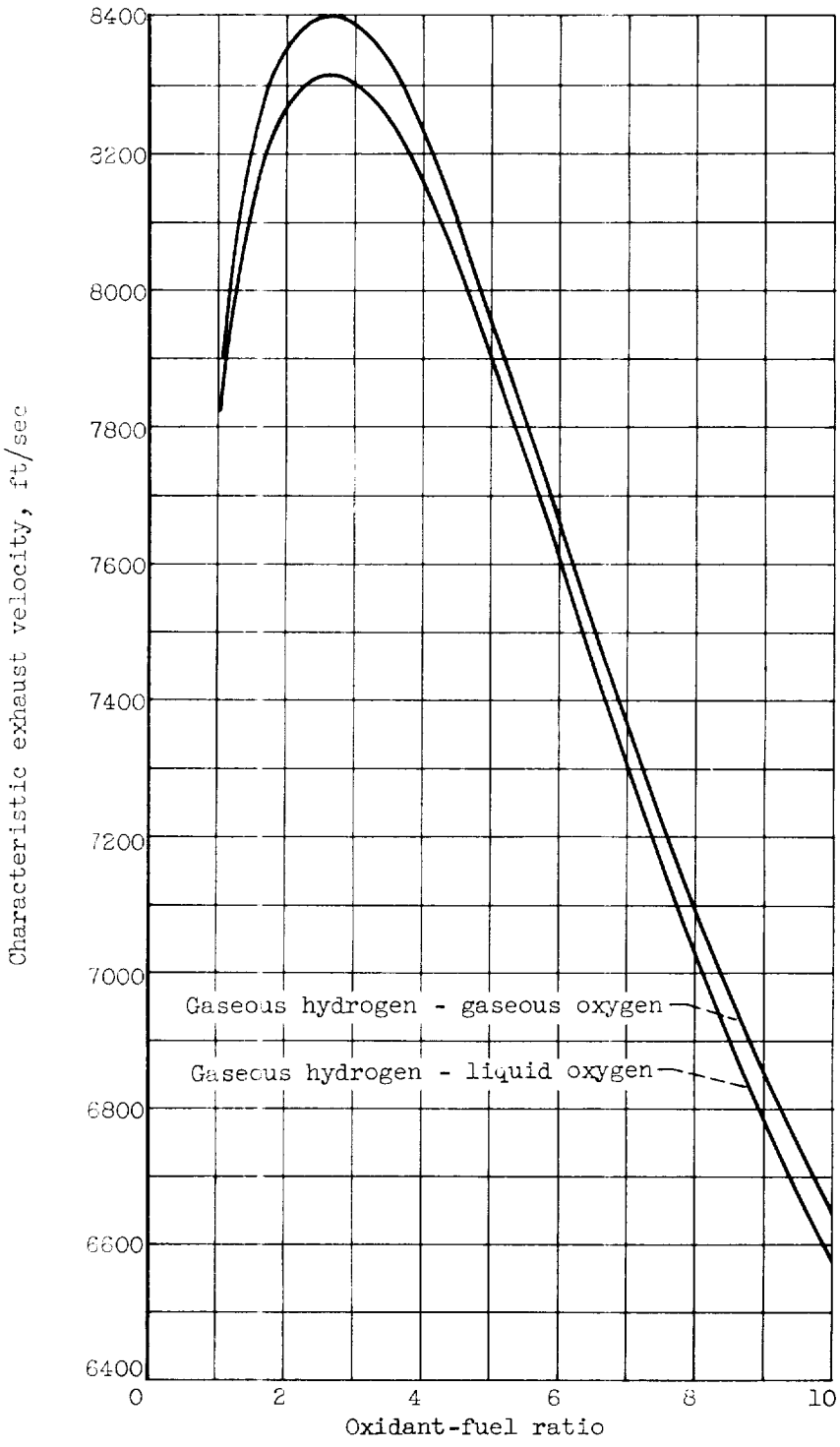

Figure 5. - Theoretical characteristic exhaust velocity as a function of oxidant-fuel ratio. Gaseous injection temperature, 298° K; chamber pressure, 300 pounds per square inch absolute.

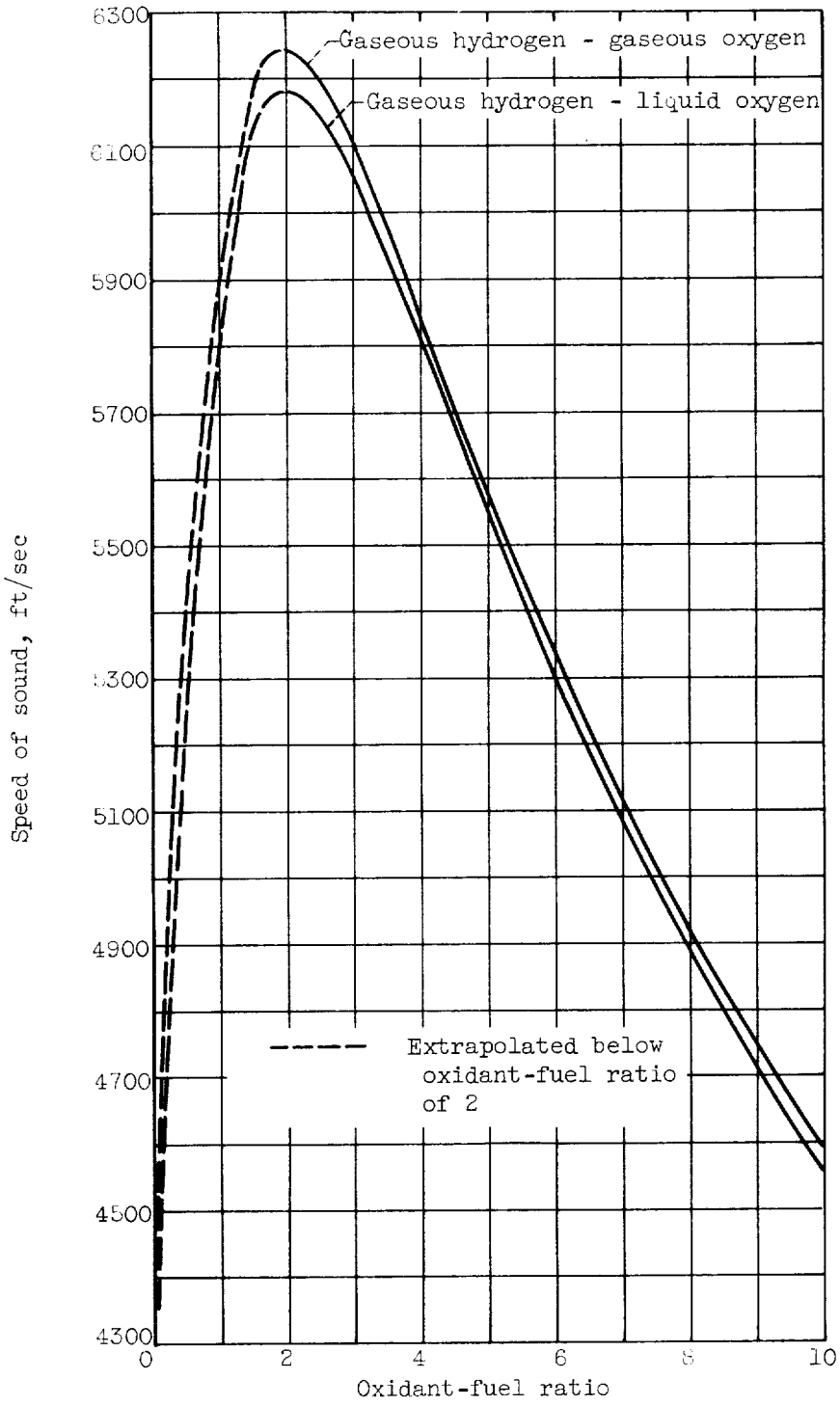

Figure 6. - Theoretical sound velocity as a function of oxidant-fuel ratio; frozen speed. Gaseous injection temperature, 298° K; chamber pressure, 300 pounds per square inch absolute.

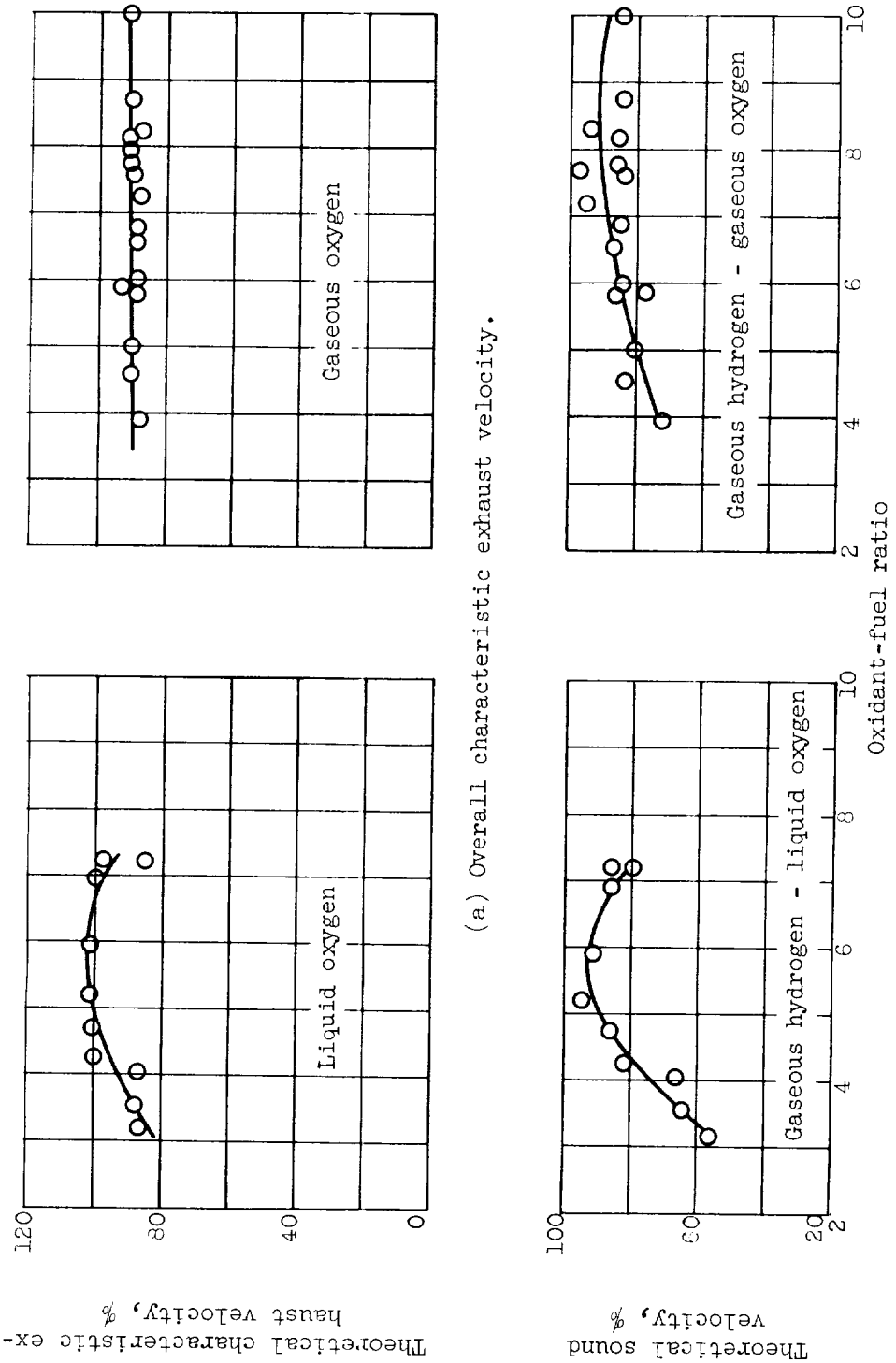

(a) Overall characteristic exhaust velocity.

(b) Sound velocity.

Figure 7. - Experimental effects of oxidant-fuel ratio on characteristic exhaust velocity and sound velocity of upstream combustion-chamber gases.

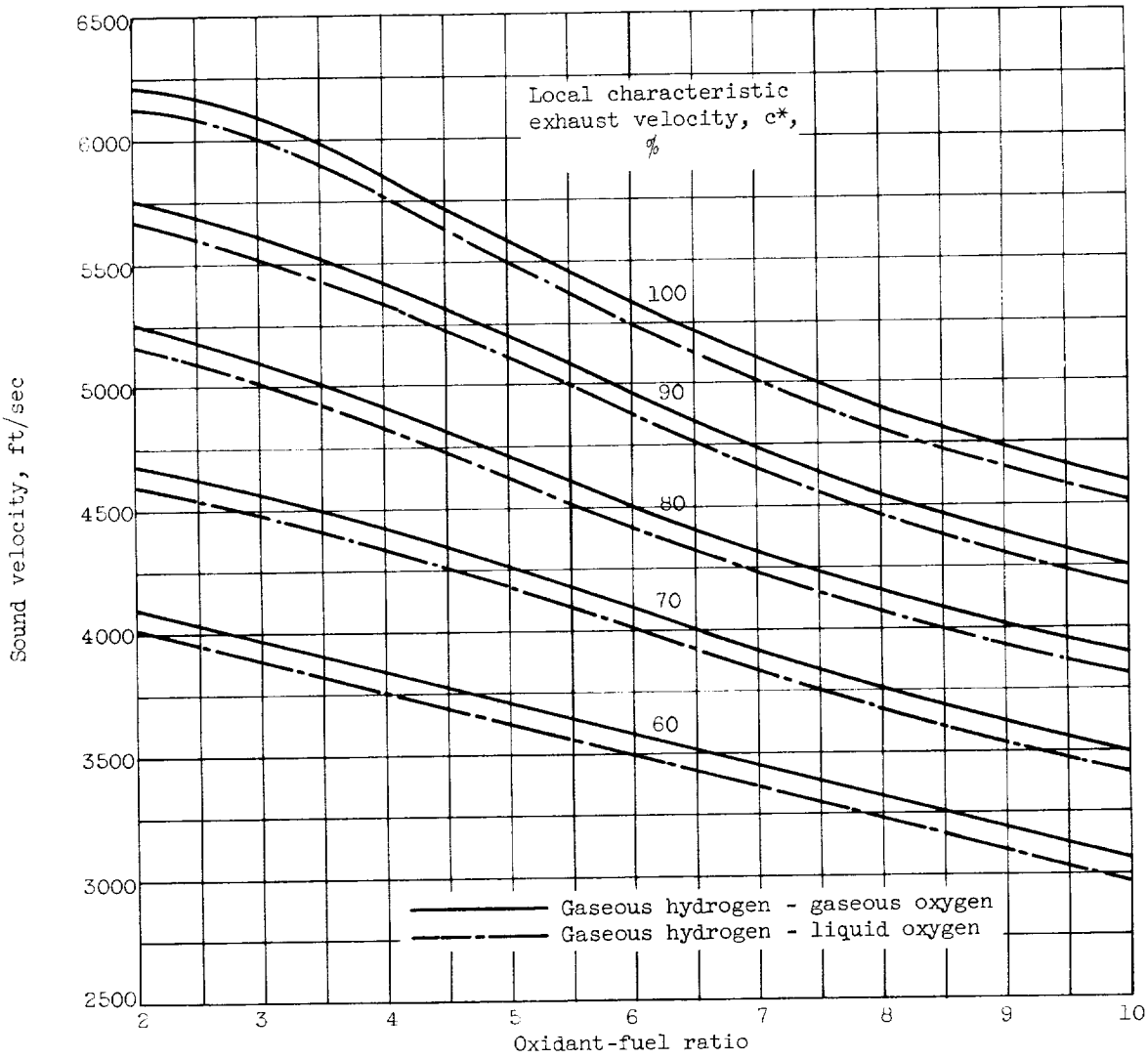

Figure 8. - Conversion of sound velocity to local characteristic exhaust velocity efficiency. Gaseous injection temperature, 298° K; chamber pressure, 300 pounds per square inch absolute.

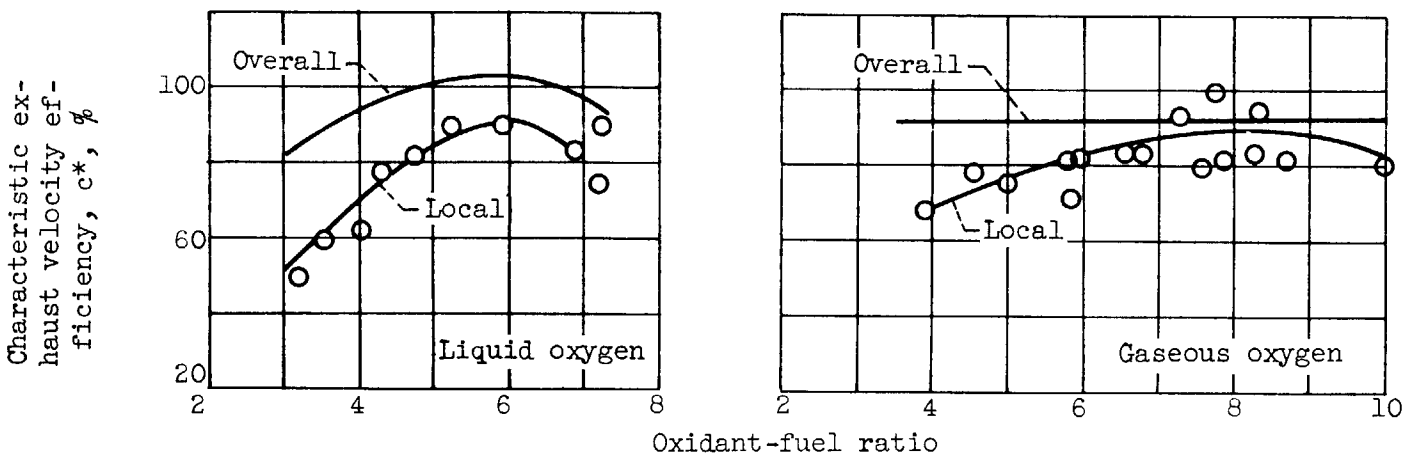

Figure 9. - Comparison of local characteristic exhaust velocity efficiency in chamber to overall characteristic exhaust velocity efficiency.

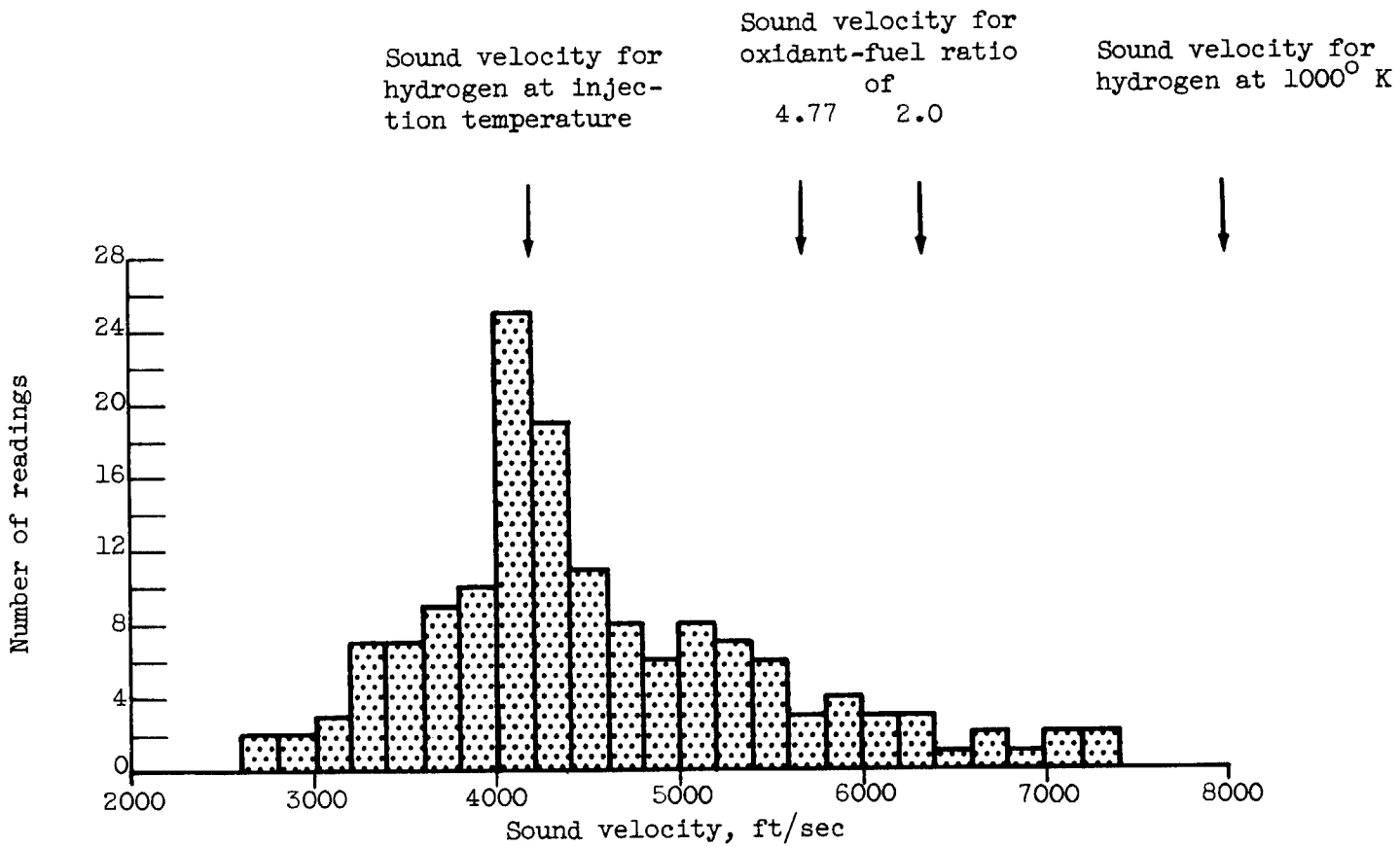

Figure 10. - Typical distribution of sound velocity measurements for a single run. Gaseous hydrogen - liquid oxygen; metered oxidant-fuel mixture, 4.77.

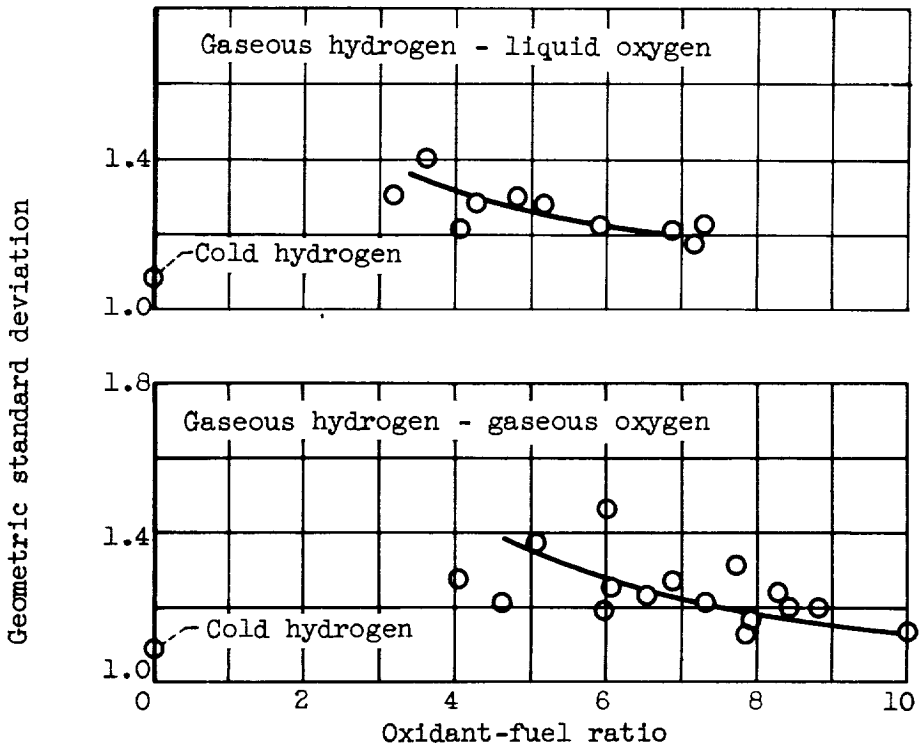

Figure 11. - Geometric standard deviation of sound velocity measurements as a function of oxidant-fuel ratio.